



ELSEVIER

Contents lists available at ScienceDirect

Atmospheric Research

journal homepage: www.elsevier.com/locate/atmosres

Performance evaluation and correction of precipitation data using the 20-year IMERG and TMPA precipitation products in diverse subregions of China

Qian Ma^{a,b}, Yi Li^{a,b,*}, Hao Feng^c, Qiang Yu^c, Yufeng Zou^d, Fenggui Liu^e, Bakhtiyor Pulatov^f

^a College of Water Resources and Architecture Engineering, Northwest A&F University, Yangling Shaanxi 712100, PR China

^b Key Laboratory of Agricultural Soil and Water Engineering in Arid and Semiarid Areas, Ministry of Education, Northwest A&F University, Yangling 712100, PR China

^c Institute of Soil and Water Conservation, Chinese Academy of Science and Ministry of Water Resources, Yangling 712100, Shaanxi, PR China

^d Institute of Water Saving Agriculture in Arid Areas of China, Northwest Agriculture and Forestry University, Yangling, Shaanxi 712100, PR China

^e Academy of Plateau Science and Sustainability, Qinghai Normal University, Xining 810016, PR China

^f Tashkent Institute of Irrigation and Agricultural Mechanization Engineers, Qoriy Niyoziy 39, 100000 Tashkent, Uzbekistan

ARTICLE INFO

Keywords:

Multi-satellite precipitation product
TMPA
IMERG
China
Climate zone

ABSTRACT

The latest Integrated Multi-satellite Retrievals for Global Precipitation Measurement (IMERG) dataset version 6, which is the successor of the multi-satellite 3B42 dataset from the Tropical Rainfall Measuring Mission Multi-satellite Precipitation Analysis (TMPA), is now recommended for many purposes. It is unclear how the quality of the latest IMERG data products compares to that of the delisted TMPA series data sets. This study evaluated the accuracy of TRMM 3B42 version 7 and IMERG final version 6 products at 677 stations in the 7 subregions of China over 2000–2019 at the daily, monthly and annual timescales based on gauge-observed precipitation data. The performance of TMPA and IMERG precipitation products was assessed by six statistical indices. The product with the best performance was corrected based on the linear relationship of monthly precipitation between remote sensing products and ground-observed precipitation. The correction was then used for the predicting and mapping of precipitation in July 2019. The results showed that (1) IMERG outperformed TMPA at all three timescales, and the accuracy increased with the expanding timescale. (2) IMERG exhibited better performance in all subregions than TMPA and performed best in the mid-temperate semihumid zone and worst in the mid-temperature arid zone. (3) IMERG showed higher accuracy than TMPA in all months for most subregions and mainland China but performed worse in dry (December, January and February) and wet (July, August and September) months. (4) The linear relationship between remote sensing products and ground-observed precipitation could be used to correct and predict satellite precipitation data without up-to-date gauge observations, the predicted map indicated the good spatial variation in precipitation and better accuracy than the original IMERG data. In conclusion, the IMERG dataset was more accurate and could be used for precipitation investigations at large scales in China.

1. Introduction

Precipitation (Pr) is a key element of the global climate and a necessary condition for the formation of regional weather. Pr is also an indispensable part of the global water cycle and the key to maintaining the balance of energy in nature (Prakash et al., 2015). Therefore, it is of great significance to understand the temporal and spatial characteristics of Pr accurately and reliably.

At present, the Pr observation methods mainly include weather radar, ground rainfall gauges, and satellite remote sensing (Jiang et al., 2014). Among these methods, ground rainfall station observations are the most common and reliable. These observations are accurate but limited to the distribution and number of stations, which are both affected by geographical conditions (Liu et al., 2011; Zhang et al., 2011a). As a result, the spatial representativeness of station observations is insufficient (Gu et al., 2010). Moreover, gridded precipitation data

Abbreviations: Pr, precipitation; TRMM, Tropical Rainfall Measuring Mission; TMPA, Tropical Rainfall Measuring Mission Multi-satellite Precipitation Analysis; GPM, Global Precipitation Measurement; IMERG, Integrated Multi-satellite Retrievals for Global Precipitation Measurement; DPR, Dual-frequency Precipitation Radar; GMI, GPM Microwave Imager; IMERG, Integrated Multi-satellite Retrievals for GPM; UTC, Coordinated Universal Time; GES DISC, Goddard Earth Sciences Data and Information Services Center; CDO, Climate Data Operator

* Corresponding author at: College of Water Resources and Architecture Engineering, Northwest A&F University, Yangling Shaanxi 712100, PR China.

E-mail address: liyili@nwfau.edu.cn (Y. Li).

<https://doi.org/10.1016/j.atmosres.2020.105304>

Received 22 June 2020; Received in revised form 3 October 2020; Accepted 5 October 2020

Available online 08 October 2020

0169-8095/ © 2020 Elsevier B.V. All rights reserved.

retrieved from interpolation methods based on gauge observations may not be reliable, especially in regions with only a few gauges and complex topography (Darand et al., 2017; Zhao et al., 2018). Compared with ground station observations, satellite remote sensing observations have certain spatial resolutions and can achieve point-to-surface expansion. The Pr information obtained by satellite technology has wider spatial coverage than that obtained by conventional observation methods. Therefore, remote sensing observations have become a preferred choice for obtaining large-scale Pr data.

The Tropical Rainfall Measuring Mission (TRMM) was launched on November 27, 1997, and was designed to improve our understanding of the distribution and variability in Pr within the tropics as part of the water cycle in the current climate system (Kummerow et al., 1998; Kummerow et al., 2000; Kidd and Huffman, 2011). Regrettably, the instruments on TRMM were turned off on April 8, 2014, and the spacecraft re-entered the Earth's atmosphere on June 15, 2015. As a successor of TRMM, the Global Precipitation Measurement (GPM) Core Observatory was launched on February 28, 2014, and provided improved estimates of light and solid Pr (Hou et al., 2014; Kirschbaum et al., 2017). The products had different temporal-spatial resolutions and time limits, were generated using multiple available sensors in the TRMM and GPM eras and were processed with TMPA (the Tropical Rainfall Measuring Mission Multi-satellite Precipitation Analysis) or IMERG (the Integrated Multi-satellite Retrievals for Global Precipitation Measurement) algorithms. A variety of versions of data sets were continuously updated in the Goddard Earth Sciences Data and Information Services Center (GES DISC). A large number of studies have shown that among satellite-retrieved precipitation products, the TMPA and IMERG products are relatively accurate for Pr measurements (Gao and Liu, 2012; Shen et al., 2010).

Previous works have assessed the performance of TMPA and IMERG products, and the results illustrated that these products have high accuracy and applicability in most studied regions and could be used in wide fields. Especially, the IMERG dataset has been improved in spatial resolution and monitoring of small precipitation than TMPA. However, since the IMERG products started after 2014, the limitation of short study periods for these studies would be a great drawback. Su et al. (2008) tested TRMM data from 1998 to 2006 in the La Plata Basin of South America. Their results showed that the daily TRMM Pr data were well correlated with the observed data, and the monthly data agreed well with the observed data with correlation coefficients > 0.95 . Asong et al. (2017) evaluated the IMERG products over different terrestrial eco-zones of southern Canada from 12 March 2014 to 31 January 2016. They found that IMERG tended to overestimate high monthly Pr over the Pacific Maritime eco-zone. Li et al. (2018) suggested that the GPM daily Pr product supplies more accurate results than near real-time products (early and late run products) and was widely adopted in hydrology and climate research. Tarek et al. (2017) analyzed the applicability of annual TRMM 3B42 V7 data in the Bengal region during 1998–2010 and commented that the TRMM data were in good agreement with the ground-station-measured Pr data. Ma and Zhao (2019) assessed the accuracy of IMERG final run products at 78 ground stations in the Tibetan Plateau from April 2014 to December 2017. They illustrated that IMERG provided more accurate Pr data when its search algorithms were improved over complex terrain and in arid regions. Yang et al. (2019) obtained a correlation coefficient above 0.85 between the TRMM 3B43 V7 and station-observed annual Pr in the Beijing-Tianjin-Hebei region from 2006 to 2015, satellite Pr data have played very important roles in characterizing the large-scale characteristics of Pr.

However, the update of the TMPA data products by GES DISC ended on December 31, 2019, and the IMERG data products are regarded as the substitute; the latest version of the IMERG dataset currently dates back to June 2000. This represents the first time that both the TRMM and GPM data are available at the same time and could both be applied in most areas. In order to better investigate the performance of the

latest dataset, the primary issue is to determine how the products perform when compared to the TMPA dataset.

Since the IMERG V06 dataset were released just recently, only a few studies have evaluated it, especially at long-term, multi-temporal scale and diverse seasons in different climate regions of mainland China. For example, Anjum et al. (2019) evaluated the IMERG V06 in the Tianshan Mountains, but the study period was just from June 2014 to December 2017. Hosseini-Moghari and Tang (2020) assessed the validity IMERG for versions 06 and compared with versions 05 products across Iran at a daily scale, but they didn't compare it with the TMPA products in multi-timescale in China. Yang et al. (2020) evaluated the accuracy of the latest IMERG V06 for hourly, daily and monthly timescales but only in the hilly Shuaishui River Basin in east-central China.

Moreover, most previous studies found that although the TMPA and IMERG data sets had good performance, there were still rectifiable errors (Darand et al., 2017; Yong et al., 2016; Mahmoud et al., 2018). Some state-of-the-art studies corrected the satellite precipitation deviation mostly on the satellite-gauge merging approaches (Lin and Wang, 2011; Wang and Lin, 2015; Wu et al., 2018; Bai et al., 2019). Previous studies found the TMPA and IMERG Pr products have good correlations with the ground-observed Pr (Wang et al., 2017; Liu et al., 2020). Hence, as a perfection and expansion of the study, using the correlation obtained from long-term satellite and ground-observed data series to correct and predict the satellite Pr without up-to-date gauge observations is useful for researchers to apply more accurate Pr data in China.

To narrow these gaps, long-term, seasonal and multi-temporal scale assessments of TMPA and IMERG in diverse climate regions of mainland China are necessary. The correction and prediction of the satellite products is useful in applications. Our objectives were (1) to investigate how the latest version of the IMERG dataset performed at daily, monthly and annual time scales and in diverse subregions of China compared with TMPA products and (2) to correct and predict the monthly satellite Pr data with the best performance based on a linear relationship between satellite products and ground-observed precipitation in China. This study provides useful guidance for the applications of IMERG products in China.

2. Materials and methods

2.1. Study area

China is located in eastern Asia, on the west coast of the Pacific Ocean, between longitudes of $E73^{\circ}41'-135^{\circ}02'$ and latitudes of $N18^{\circ}10'-53^{\circ}33'$, with a land area of 9.659 million km^2 . Due to the obvious influence of the monsoon climate and complex terrain, the spatio-temporal distribution of Pr is uneven, with low values in western regions and winter and high values in eastern regions and summer. Since there are typical differences in seasonal and regional Pr (Zhang et al., 2011b), China is divided into 7 climate zones (Zhang, 1983). The climatic characteristics and average annual Pr information for each sub-region are given in Table 1.

2.2. Data

Two satellite datasets, namely, TRMM 3B42 V07 and GPM IMERG final V06, obtained from GES DISC were selected and verified by ground-station-measured Pr information to analyze and compare their applicability in diverse subregions and time periods.

2.2.1. Station-observed precipitation data

The ground-station-observed daily Pr data at the 839 meteorological stations were collected from the China Meteorological Data Network (<http://data.cma.cn>), and a total of 677 sites were selected to guarantee the integrity of the Pr series with missing ratios limited to 1% from June 1, 2000 to June 30, 2019. Missing data were interpolated from 10 most

Table 1
The climatic characteristics and average annual Pr information of the seven subregions.

Subregions	I	II	III	IV
Climate	Mid-temperate arid	Mid-temperate semiarid	Plateau sub-frozen semiarid	Mid-temperate semihumid
Average Pr (mm year ⁻¹)	175.95	321.89	511.98	598.02
Subregions	V	VI	VII	
Climate	Warm temperate semihumid	North subtropical humid	Tropical humid	
Average Pr (mm year ⁻¹)	571.02	1422.47	1707.99	

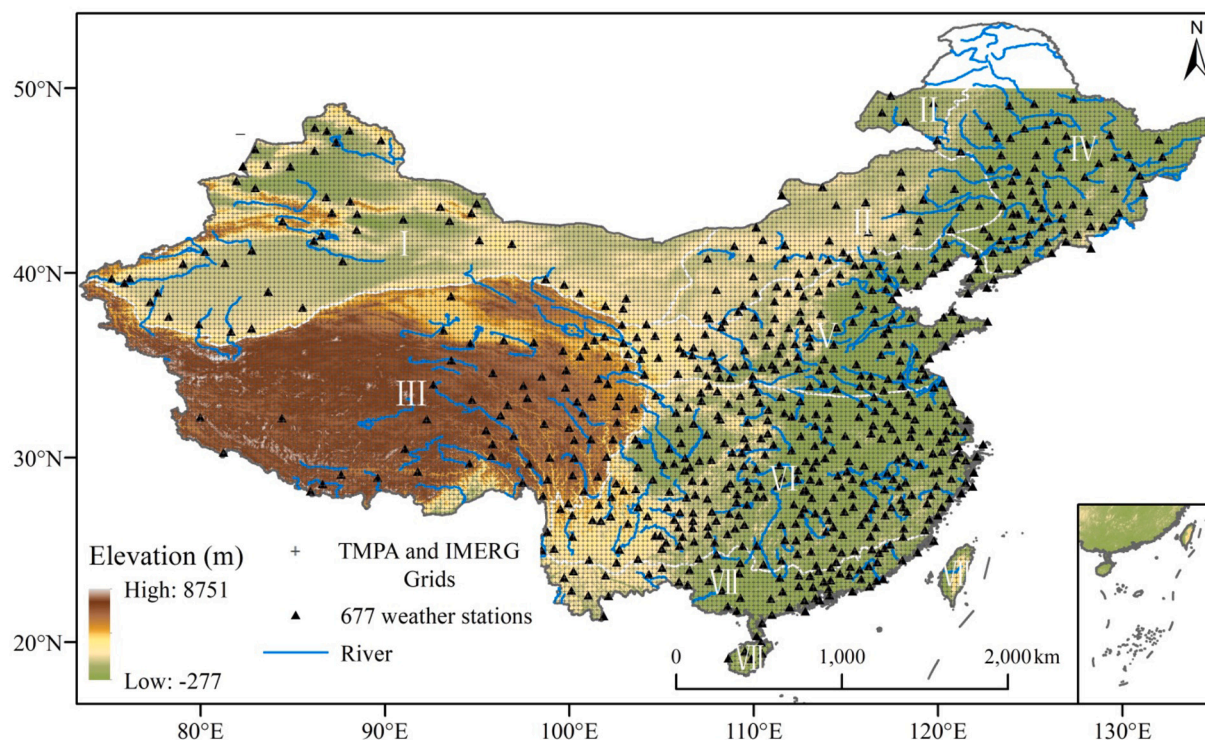


Fig. 1. Map of weather stations, digital elevation and TMPA and IMERG grids in China.

adjacent sites collected on the same calendar day. The observation data were subjected to strict quality control, including climate limit value inspection, station extreme value inspection, and spatiotemporal consistency inspection using nonparametric tests, including the Kendall autocorrelation test and Mann-Whitney homogeneity tests (Helsel and Hirsch, 1992). The daily Pr data were recorded from 8:00 to 8:00 of the next day in Beijing time (8 h ahead of coordinated universal time (UTC) time), so in UTC time it was from 00:00 to 24:00, which synchronize with the satellite data. The digital elevation model of China and the locations and distribution of weather stations are shown in Fig. 1.

2.2.2. TMPA data

The TRMM satellite was launched in 1997 as a joint space mission between the National Aeronautics and Space Administration (NASA) and the Japanese Aerospace Exploration Agency (JAXA) to provide satellite-based monitoring of global Pr (Zhao et al., 2015), flying at a low orbital altitude of 240 miles (400 km), with several instruments to detect rainfall, including radar, microwave imaging, and lightning sensors; unfortunately, it was turned off on April 8, 2015, with the spacecraft reentering the Earth's atmosphere on June 15, 2015. Although TRMM terminated, the multisatellite TMPA data sets that continued to update could be retrieved from January 1998 to the present using input data from other satellites in the constellation.

Since the algorithm applied in the TRMM series is the Version 7

TRMM Multi-satellite Precipitation Analysis (Huffman et al., 2007, 2010), the datasets are called "TMPA". Within the TMPA datasets, 3B42 processing is designed to maximize data quality and is strongly recommended for many studies. The TRMM 3B42 V07 dataset is freely available at (disc.gsfc.nasa.gov) with spatial coverage from -180° , -50° to 180° , 50° and temporal coverage from 1998 to 01-01 to 2019-12-31. In the current study, Pr estimates obtained from TRMM 3B42 V07 were used from June 30, 2000, to June 30, 2019, with a spatial resolution of $0.25^{\circ} \times 0.25^{\circ}$ and temporal resolution of 1 day, which were recorded from 0:00 to 24:00 in UTC (processed by accumulating 3-h TMPA products between 00:00 to 24:00, which is consistent with ground-station-observed and IMERG Pr recording time). The monthly and annual data were cumulated from the daily data product.

2.2.3. IMERG data

The GPM is an international satellite network that was built upon the success of TRMM. GPM has approximately 10 constellation satellites and a "core" satellite that was launched on February 27, 2014, from the Tanegashima Space Center, Japan, carrying the multi-channel GPM Microwave Imager. The GMI utilizes a set of frequencies and the first space-borne Ku/Ka-band dual-frequency Pr radar as a reference standard to unify Pr measurements from a constellation of research and operational satellites. The frequencies have been optimized over the past two decades, and the DPR is highly sensitive to light rain rates and

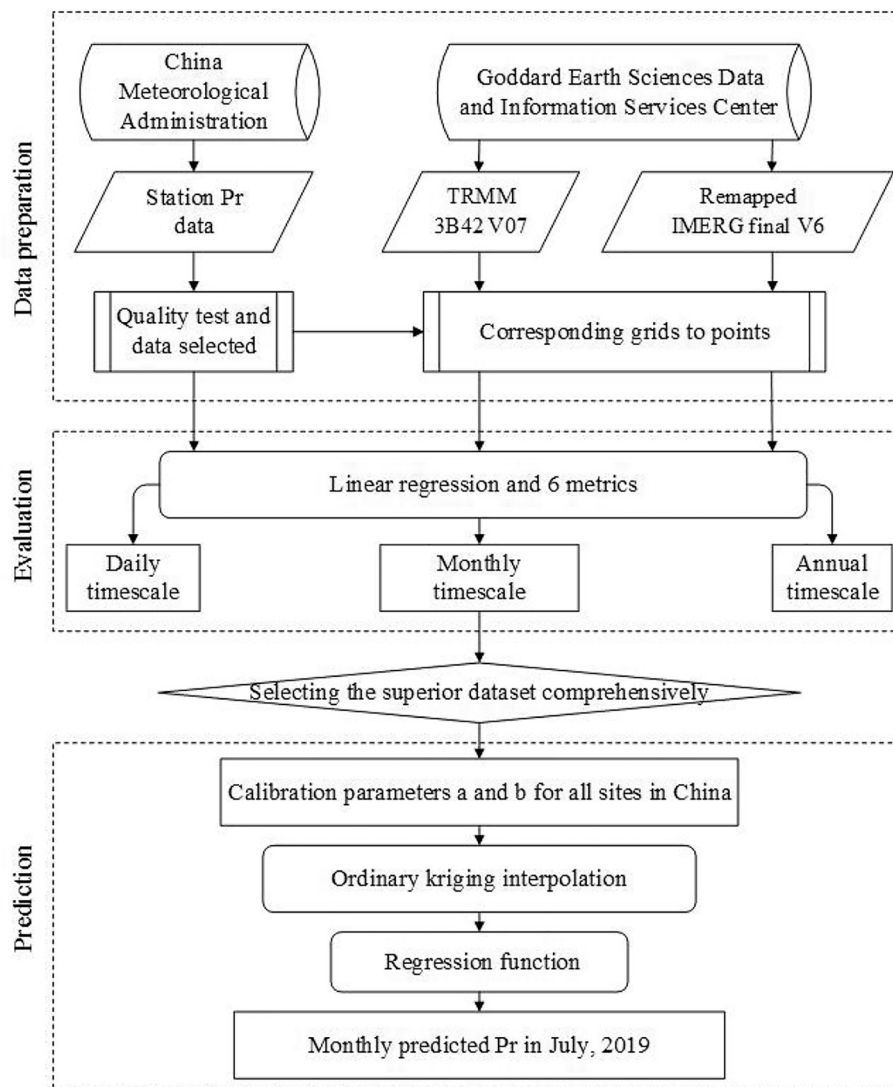


Fig. 2. The main flowchart of this research.

snowfall (Hou et al., 2014).

The IMERG algorithm applied to the product is designed for inter-calibrating, merging, and interpolating “all” satellite microwave Pr estimates, including microwave-calibrated infrared satellite estimates, together with sedimentation analysis and potential Pr estimates at fine temporal and spatial scales for the TRMM and GPM eras over the entire globe. Currently, IMERG final V06 was retrospectively processed back through the TRMM era, initially starting in June 2000 and continuing to present. This product has a fine spatial resolution of $0.1^\circ \times 0.1^\circ$, spatial coverage from 60°S to 60°N , was recorded from 0:00 to 24:00 in UTC, was derived from the half-hourly GPM_3IMERGHH, and was released after an approximately two- or three-month delay in the final estimate of the real-time daily cumulative Pr (https://disc.gsfc.nasa.gov/datasets/GPM_3IMERGDF_V05/) (Li et al., 2018).

The research period of evaluation was from June 1, 2000, to June 30, 2019, and the duration of the prediction was July 2019.

To maintain the consistency of the spatial resolution with TMPA (Tang et al., 2016; Ma et al., 2016), the resampled IMERG data were obtained from Goddard Earth Sciences Data and Information Services Center (GES DISC) with a resolution of $0.25^\circ \times 0.25^\circ$, which was created using a distance-weighted remapping of the four nearest neighbor values of fields between grids in spherical coordinates with the Climate Data Operator (CDO) software (Zender, 2008); the specific process of data computation is shown at the website (<https://code.mpimet.mpg.de/projects/cdo> embedded/cdo.pdf).

<https://code.mpimet.mpg.de/projects/cdo> embedded/cdo.pdf).

2.3. Methodology

2.3.1. Resampling of Pr for the grids of satellite data

Since interpolating the station-observed data to spatial values may have caused some errors (Jin et al., 2016), this study compares and evaluates the accuracy of TMPA and IMERG Pr data based on the scale of stations. The coordinates of the meteorological stations are used to extract the satellite Pr data from the corresponding grid (Chen et al., 2018). The station-observed Pr data were averaged if there was more than one site in each grid. In addition, if the station coordinates fell on the boundary lines between two grids, then the Pr data from both satellite grids that contain the ground station were used.

2.3.2. Evaluation of the performance of TMPA and IMERG products

Six indicators are selected for assessing the data-retrieving performance: root mean square error (RMSE), relative bias (RB), relative root mean square error (RRMSE), coefficient of determination (R^2), detection rate (POD), false alarm ratio (FAR) and critical success index (CSI).

$$\text{RMSE} = \sqrt{\frac{\sum_{i=1}^n (S_i - G_i)^2}{n}} \quad (1)$$

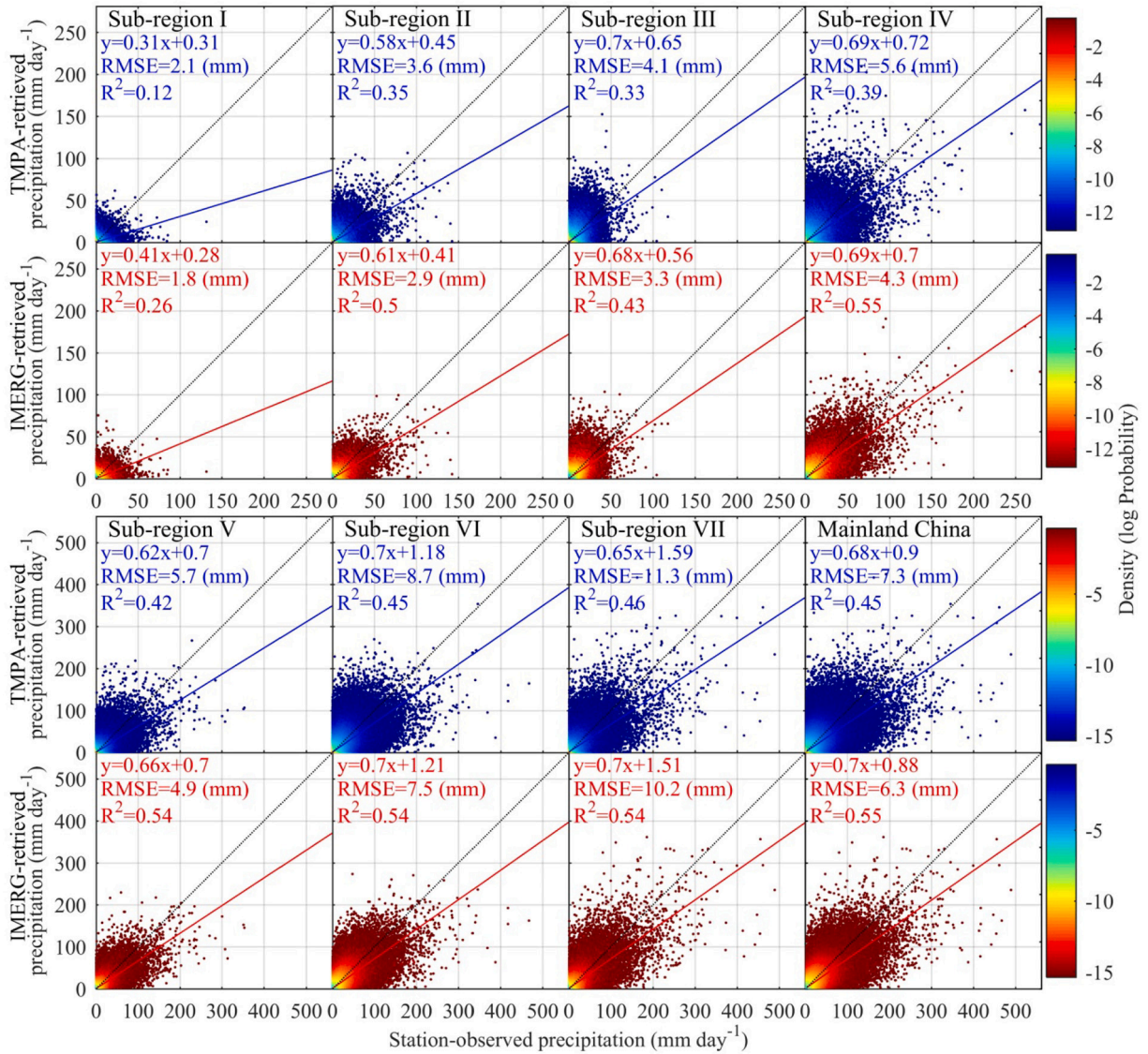


Fig. 3. Density scatter plots of gauge-measured versus TRMM- or IMERG GPM- retrieved daily Pr values in different subregions and mainland China from June, 1, 2000 to June, 30, 2019.

$$RB = \frac{\sum_{i=1}^n (S_i - G_i)}{\sum_{i=1}^n G_i} \quad (2)$$

$$RRMSE = \sqrt{\frac{\sum_{i=1}^n (S_i - G_i)^2}{n}} \cdot \frac{1}{\sum_{i=1}^n G_i} \quad (3)$$

$$POD = \frac{H}{H + M} \quad (4)$$

$$FAR = \frac{F}{H + F} \quad (5)$$

$$CSI = \frac{H}{H + M + F} \quad (6)$$

where n represents the number of stations; S_i and G_i represent satellite-retrieved and station-observed Pr (mm), respectively; H represents observed rain correctly detected; M represents observed rain not detected; F represents rain detected but not observed (detailed explanations of POD, FAR, and CSI are provided in Ebert et al. (2007) and generally suitable for daily scale). The six evaluation parameters can reflect the performance of satellite products. For example, better

performance is obtained when the $RMSE$, $RRMSE$ and RB are close to 0 or the R^2 value is close to 1. The higher the POD value is, the smaller the leakage rate of satellite Pr data. As FAR values are close to 1, there is low error in the satellite data. The larger the CSI value is, the stronger the comprehensive prediction ability of satellite data.

Three timescales of daily, monthly, and yearly are compared for the two satellite products. The comparison between TMPA, IMERG and station-observed data is conducted at each station, in 7 subregions and over mainland China, for the daily, monthly and annual timescales, particularly in different months.

2.3.3. Calibration and validation of precipitation based on satellite products

In order to correct and predict the satellite products, linear regression analysis is conducted for each station between pairs of the TMPA, IMERG, and ground-station-measured Pr using the 20 years of data to obtain the calibration parameter a and b . The relationship is written as follows:

$$Pr_{obs} = a Pr_{sat} + b \quad (7)$$

where Pr_{sat} is satellite-retrieved Pr; Pr_{obs} is station-observed Pr, a is slope and b is intercept. To compare the performance of the two satellite

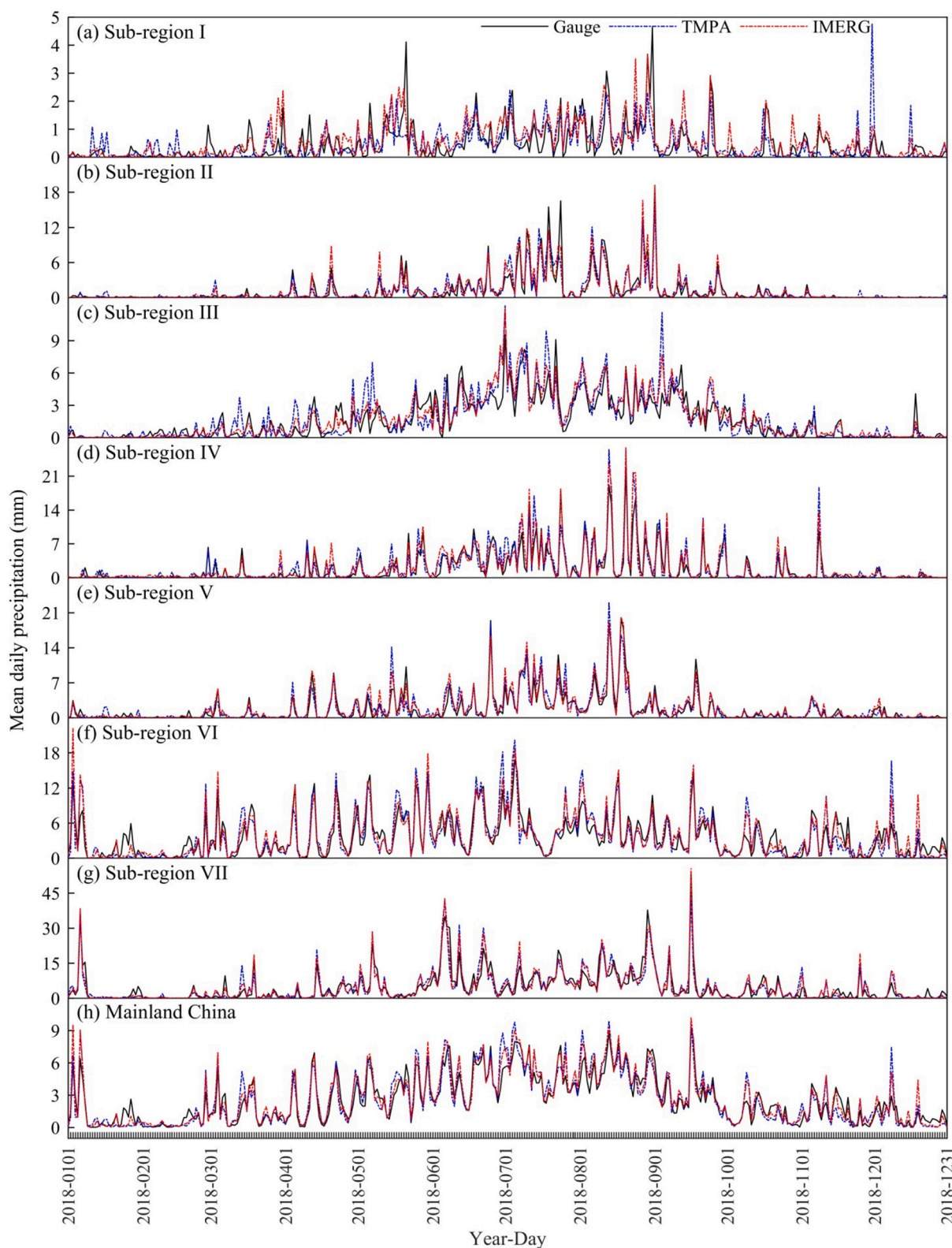


Fig. 4. Comparison of the temporal variations of the observed, TMPA- and IMERG- retrieved mean daily Pr in 2018 for different subregions and mainland China.

products and assess the reliability of calibration parameters, the R^2 value is obtained. Only the monthly timescale is evaluated using Eq. 7.

To validate the reliability of prediction with observed stations, the monthly Pr from June 2000 to May 2017 was chose for calibration and the remain was used for validation.

2.3.4. Prediction of monthly precipitation

The parameters a and b in Eq. 7 could be further utilized to predict the satellite Pr data, which have been validated and showed better performance in different months of the coming years for all grids in mainland China. Based on previous researches (Dinku et al., 2010; Wehbe et al., 2017; Macharia et al., 2020), the ordinary kriging method

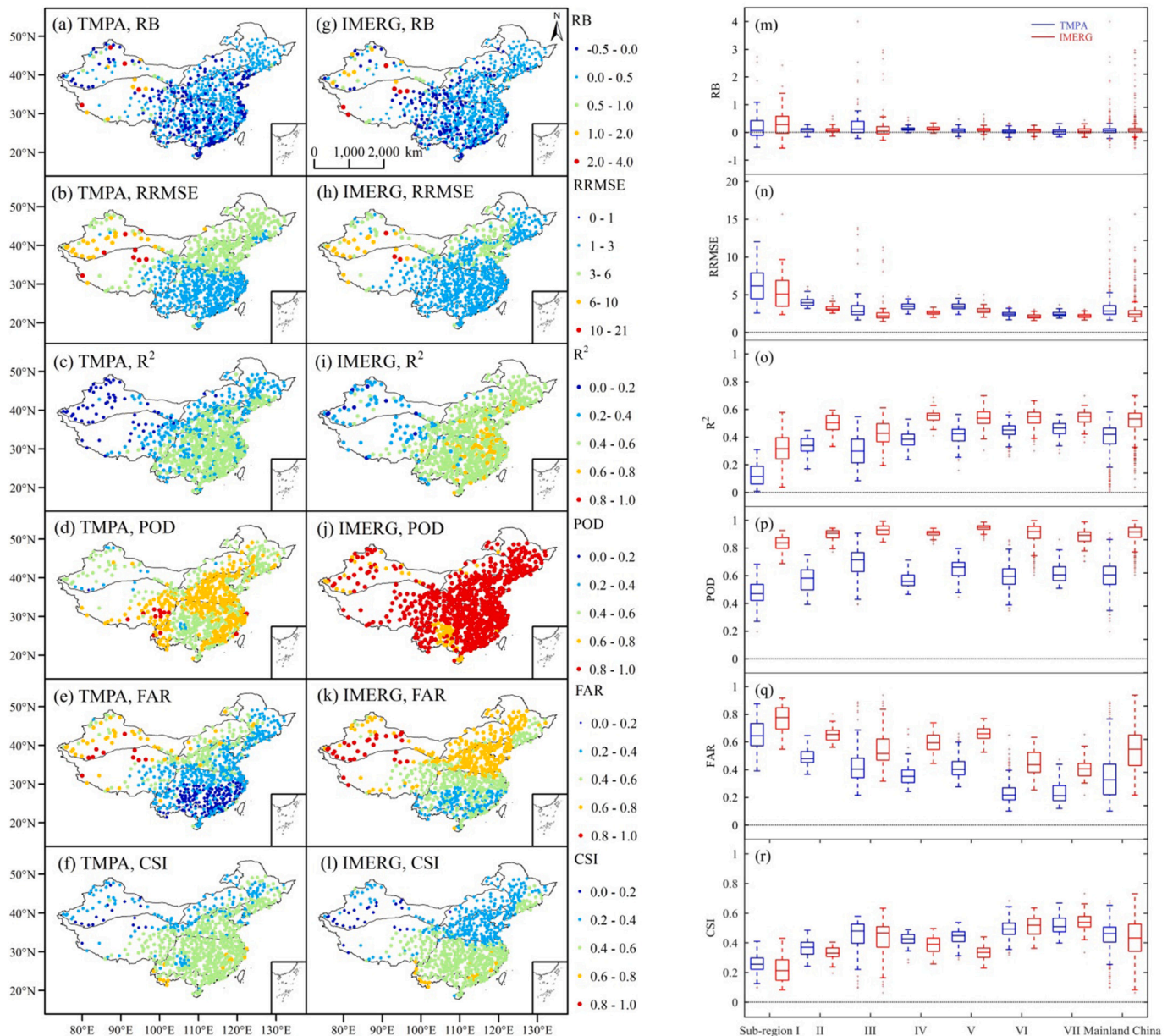


Fig. 5. Spatial distribution of RB, RRMSE, R², POD, FAR and CSI in China and boxplots in different subregions from June, 1, 2000, to June, 30, 2019.

is chosen to interpolate parameters *a* and *b* from sites to grids at a resolution consistent with that of the satellite data. Then, the monthly satellite Pr could be predicted in the studied area of China using the relationship of Eq. 7, namely, $Pr_{pre} = aPr_{sat} + b$.

Ten-fold cross-validation was conducted for prediction of Pr after interpolation. The Nash–Sutcliffe efficiency (NSE) and standard error of estimates (SEE) were selected to characterize the validation performance (Nash and Sutcliffe, 1970; Gravetter and Wallnau, 2006):

$$NSE = 1 - \frac{\sum_{i=1}^n (Pr_{obs} - Pr_{pre})^2}{\sum_{i=1}^n (Pr_{obs} - \bar{Pr}_{obs})^2} \quad (8)$$

$$SEE = \sqrt{\frac{\sum_{i=1}^n (Pr_{pre} - Pr'_{obs})^2}{n - 2}} \quad (9)$$

where *n* represents the total number of stations; Pr_{obs} is station-observed Pr; Pr_{pre} is predicted Pr; \bar{Pr}_{obs} is mean station-observed Pr; Pr'_{obs} is stations-observed Pr representing the regression line. NSE ranges from $-\infty$ to 1. Values of NSE within the range 0–1 are considered acceptable,

NSE < 0 are unacceptable, $N = 1$ means perfect. The smaller the SEE value, the less deviations of the predicted Pr from regression line.

The main idea and procedure of this research is illustrated in Fig. 2.

3. Results

3.1. Performance of the TMPA- and IMERG-retrieved Pr products

3.1.1. At the daily timescale

The satellite-retrieved Pr values at the daily timescale from June 1, 2000, to June 30, 2019, were compared with the ground-station-observed Pr values. The density scatter plots and their correlations are illustrated for different subregions (including data from all sites in the region) and mainland China (total number of sites is 677) in Fig. 3. In general, both TMPA and IMERG underestimated daily Pr as the regressive function lines were mostly below the 1:1 line. The plots showed low accuracy of both the TMPA and IMERG Pr products at the daily scale. The coefficients of determination (R^2) were not high, ranging from 0.15 to 0.46 for TMPA and from 0.26 to 0.55 for IMERG. The

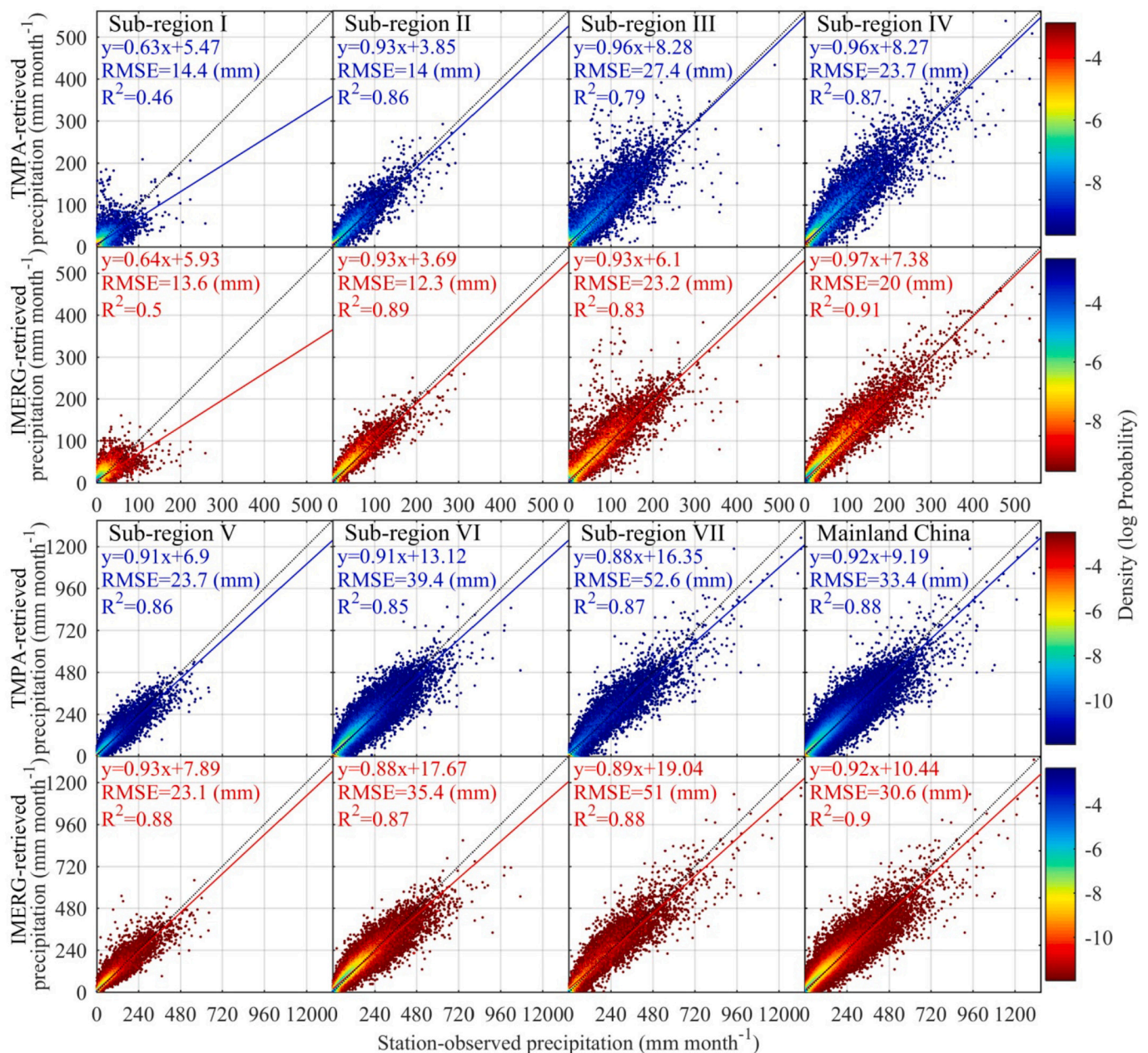


Fig. 6. Density scatter plots of gauge-measured versus TMPA- or IMERG- retrieved monthly Pr values in different subregions and mainland China from June 2000 to June 2019.

IMERG daily Pr, which had lower RMSE and higher R² values than the TMPA data, showed slightly better performance in different subregions and mainland China. The linear slope, intercept, RMSE and R² values varied smoothly for most subregions except subregion I, which exhibited remarkably poor accuracy since Pr was generally low.

The temporal variations in the IMERG- and TMPA-retrieved mean daily Pr values were compared with the observed values in different subregions and mainland China to show the differences clearly. Only daily Pr values in 2018 are shown (Fig. 4), of which the mean daily Pr values were calculated by averaging the observed and corresponding satellite-retrieved Pr values from all the stations in the subregion. Both IMERG and TMPA captured the main variation patterns, and their general Pr variations did not deviate from the gauge-observed daily Pr greatly in subregions II, IV, V, VI, and VII and mainland China. TMPA deviated more from the gauge data than IMERG in subregions I and III, where precipitation was low (< 5 mm day⁻¹), but neither captured the

peak values very well. In subregion I, both IMERG and TMPA exhibited low consistency with the observed Pr, especially in the dry months, when Pr values were low. In subregion III, IMERG agreed with the observed daily Pr prominently better than TMPA. The deviation fluctuated with the month. The radar plots of RB, RRMSE, R², POD, FAR and CSI of the two satellite products for 12 months are illustrated in Fig. S-1. Generally better performance in wet months and worse performance in dry months were shown for both satellites, and IMERG outperformed TMPA for all months. For mainland China, both products performed well by visual comparison, especially IMERG.

The spatial distributions of the six statistics (RB, RRMSE, R², POD, FAR and CSI) used to evaluate the accuracy of TMPA- and IMERG-retrieved daily mean Pr at all 677 sites are mapped in Fig. 5. The RB, RRMSE, R², POD, FAR and CSI varied with different sites but still had regional characteristics (Figs. 5a to 5l). The RB values were mostly positive and generally low in eastern China but were negative in central

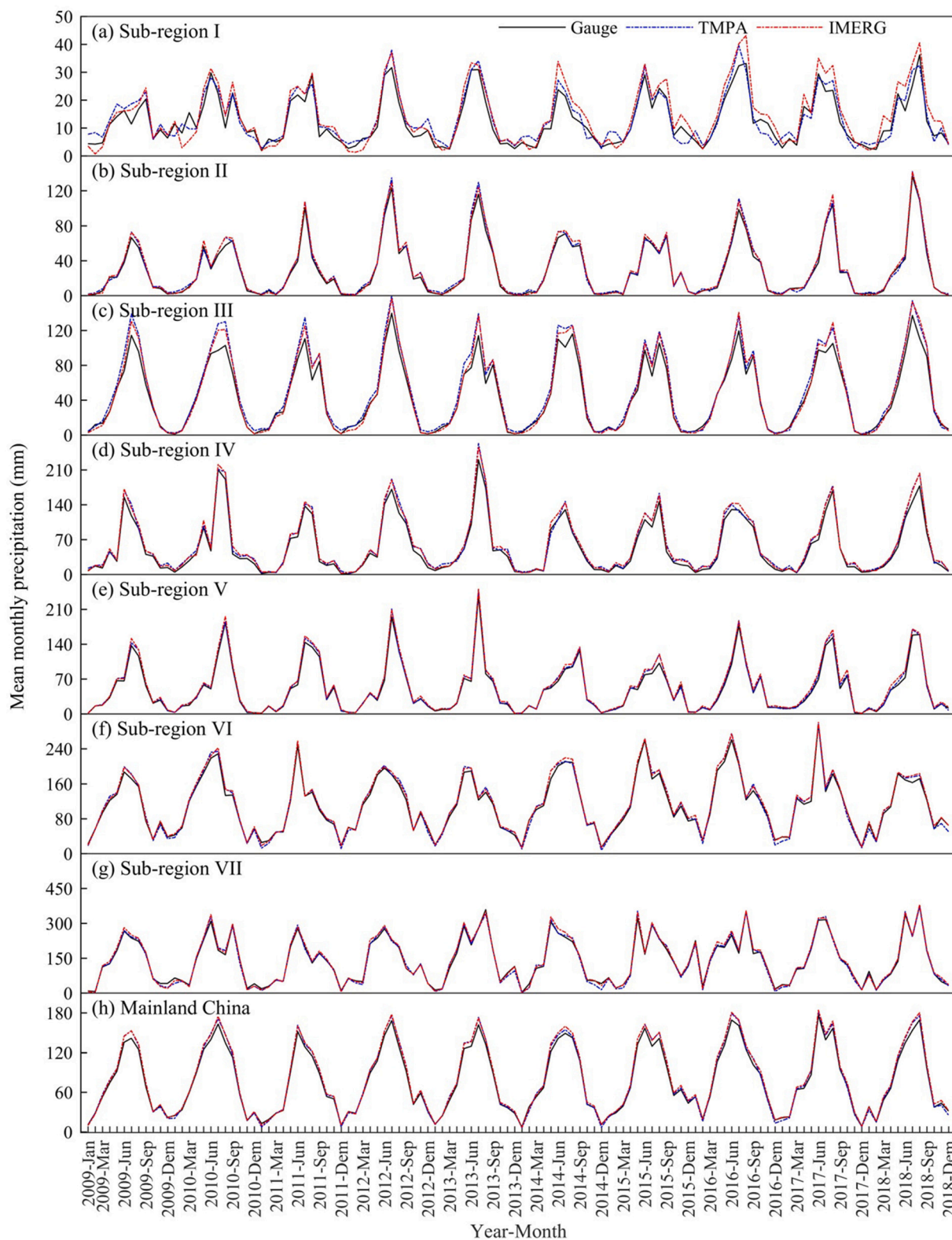


Fig. 7. Comparison of the temporal variations in the observed and TMPA- and IMERG-retrieved mean monthly Pr (from January 2009 to December 2018) in different subregions and mainland China.

south China (Fig. 5a and g). The *RRMSE* values for IMERG were commonly lower than those for TMPA and were generally positive in southern China (Fig. 5b and h). The values of R^2 were all positive but generally large in eastern China (Fig. 5c and i). The *POD* values for IMERG were generally larger than those for TMPA (Fig. 5d and j). The

FAR values of IMERG were higher than those of TMPA and decreased with decreasing latitude (Fig. 5e and k). The *CSI* values of TMPA were slightly larger than those of IMERG and higher in southern China (Fig. 5f and l). For the 7 subregions, IMERG had small values and ranges of *RB* in all subregions except subregion I (arid and semiarid regions)

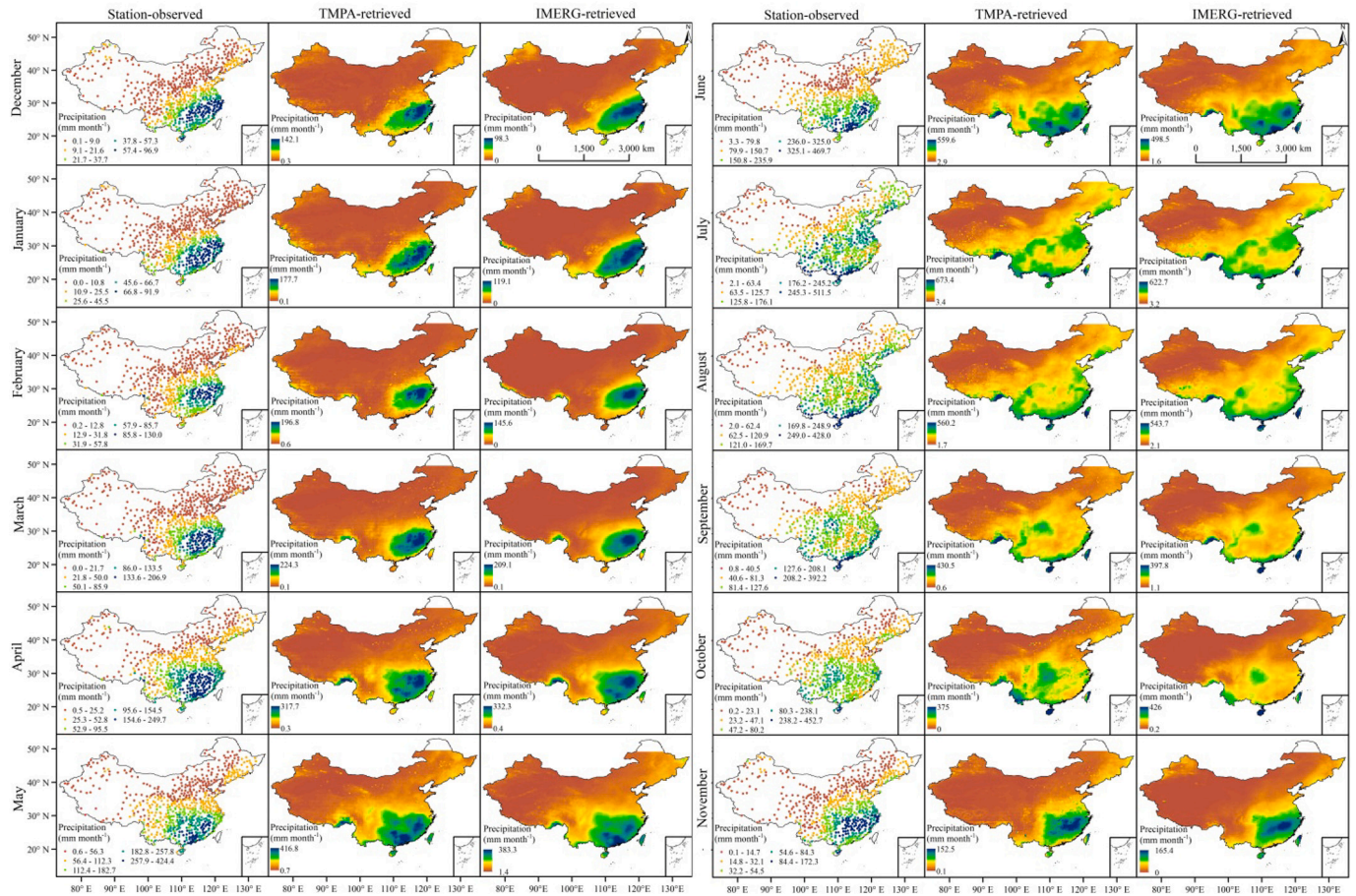


Fig. 8. Spatial distribution of station-observed and TMPA- and IMERG-retrieved monthly Pr in China (averaged from June 2000 to June 2019).

(Fig. 5m). For most of the subregions except I, the *RRMSE* values for IMERG were low (Fig. 5n). The R^2 and *POD* values of IMERG were obviously larger than those of TMPA in the 7 subregions, especially in subregion I (arid and semiarid regions) (Fig. 5o and p). The highest *FAR* values occurred in subregion I, and the lowest *FAR* value was in subregion VI (Fig. 5q). Except for in subregions VI and VII, TMPA had higher *CSI* values than IMERG (Fig. 5r). In general, the performance of IMERG was better than that of TMPA.

3.1.2. At the monthly timescale

The density scatter plots of the observed and satellite-retrieved monthly Pr for different climate zones and throughout mainland China are shown in Fig. 6. The performances of the TMPA- and IMERG-retrieved monthly Pr were much better than those at the daily timescale, with R^2 values generally larger than 0.79 (except for the R^2 values in subregion I). The regressive lines were close to the 1:1 line, and the values ranged from 0.88–0.97 for subregions II to VII and mainland China. The *RMSE* values of IMERG were all smaller than those of TMPA in all 7 subregions and mainland China. The spatial distribution of the six evaluation metrics is shown in Fig. S-2 but is not described in detail here.

The mean values of the observed and TMPA- and IMERG-retrieved monthly Pr in different subregions and mainland China are compared for the last 10 years in Fig. 7. The periodic changes in monthly Pr were visually observed from all three lines. Both the IMERG- and TMPA-retrieved monthly Pr values were visually close to the observed Pr data, and both showed very similar fluctuation patterns in different subregions. The deviations of both satellite-retrieved Pr values were large in semiarid and arid subregions (I to III) but generally small in wet regions (IV to VII). For subregions I and III, neither IMERG nor TMPA

precisely captured peak and valley monthly Pr values, especially from January to March and November to December. Comparatively, the IMERG values seemed larger than the gauge-measured Pr values and TMPA-retrieved values; however, it maintained a similar pattern with the observed Pr values. This result would be a very useful feature for upscaling Pr data. In addition, when compared to the daily scale, both the IMERG and TMPA products showed improved performance. A detailed comparison with the gauge-observed monthly Pr values showed that in most cases, the IMERG data performed better than the TMPA data, except in February and March for subregions I and V. A more detailed comparison of the satellite-retrieved monthly Pr with the ground-station-observed values in the 12 months of the year for different subregions and mainland China is plotted in Fig. S-3. The differences in performance varied with month and generally agreed well with Fig. 6 for different subregions, namely, IMERG performed better than TMPA.

The spatial distribution of the average monthly Pr estimated from station-observed data and TMPA- and IMERG-retrieved data in China were compared over 12 months (Fig. 8). In general, both products reflected the spatial Pr distribution patterns and overcame the shortage of station-based results. In the meantime, both the TMPA- and IMERG-retrieved Pr products showed local underestimation in May, October and November. The spatial distribution of the IMERG-retrieved monthly Pr exhibited the best performance for most months except April and May.

3.1.3. At the annual timescale

The density scatter plots of the observed and satellite-retrieved annual Pr for different subregions and mainland China are shown in Fig. 9. The TMPA- and IMERG-retrieved annual Pr deviated from the

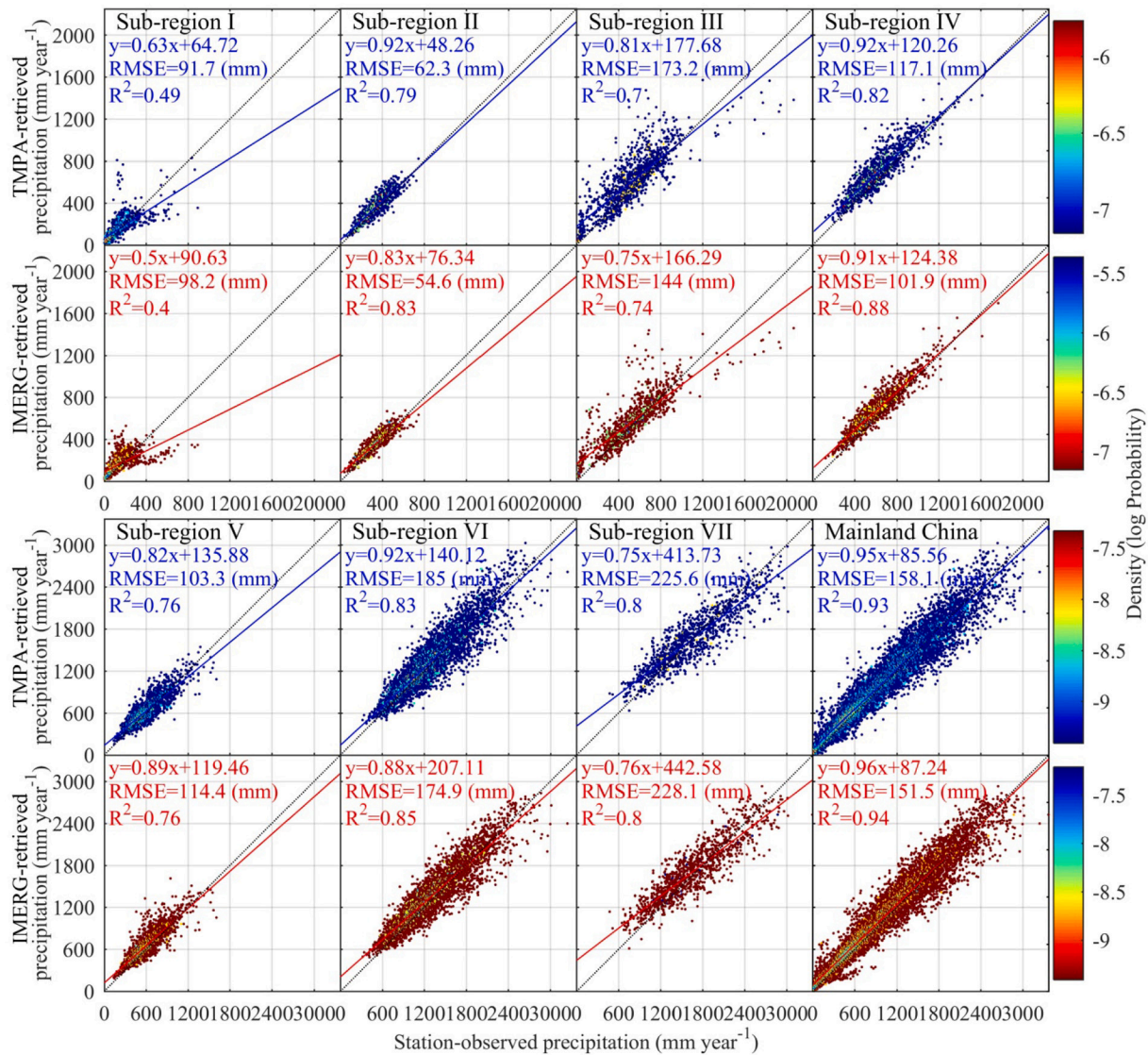


Fig. 9. Density scatter plots of gauge-measured versus TMPA- or IMERG- retrieved annual Pr values in different subregions and mainland China from 2001 to 2018.

observed values more in subregion I ($0.39 < R^2 < 0.5$) than in the other subregions ($0.70 < R^2 < 0.94$). The IMERG data performed better than TMPA for most of the subregions. For mainland China, both performed very well.

To compare the temporal variations, the gauge-observed and TMPA- and IMERG-retrieved annual Pr over 2001–2018 in different subregions and mainland China are illustrated in Fig. 10. For subregion I, the IMERG-retrieved annual Pr values were closer to the observed values than the TMPA-retrieved annual Pr values before 2013, and IMERG widely deviated from the observed Pr after 2013. For subregions II, III, and IV, the deviations of the two satellite-retrieved Pr curves were larger than those for subregions V, VI and VII, and IMERG generally had lower deviations than TMPA, which was especially obvious for subregion III. For subregions V, VI, and IV, the deviations of the two satellite-retrieved Pr curves from the gauge-observed Pr curves were both small over the period, and TMPA performed slightly better than IMERG. Overall, both satellite-retrieved Pr values had similar fluctuation patterns with the observed values. By comparing *RB*, *RRMSE* and *R²* (Fig. S-4), the two satellite products exhibited very similar spatial distributions of performance (Fig. S-4a), and IMERG performed slightly better than TMPA, especially in northwestern China (subregions I and II) (Fig. S-4b).

For a direct comparison of the performance of satellite products for

different subregions and different timescales, the *RRMSE* and *R²* values are presented in Table 2. The *RRMSE* showed improved performance as the timescale increased from daily to yearly, while the *R²* showed that the monthly scale exhibited better performance than the daily and yearly scales. The IMERG data showed lower biases and higher correlations with the gauge-observed Pr than the TMPA data for most subregions and mainland China. Therefore, IMERG data could be further utilized to correct and predict Pr in China.

3.2. Prediction of monthly Pr in mainland China

According to the above accuracy evaluation results, IMERG-retrieved Pr data exhibited better performance than TMPA at the daily, monthly, and annual timescales and in most subregions. In particular, IMERG Pr at the monthly timescale showed higher accuracy than that at the other timescales. Thus, monthly IMERG Pr data could be applied for Pr prediction based on the calibrated *a* and *b* parameters in Eq. 7 over 2000–2017 (Figs. 11). The parameters *a* and *b* varied within ranges of 0.3–1.0 and -25.3 to 35.7 in China. At most sites in eastern China, IMERG-retrieved products showed good performance ($R^2 \geq 0.6$). Approximately 607 sites of the total 677 sites had good performance ($R^2 \geq 0.80$). Even in northwestern China, where the *R²* values were low, most *R²* values were approximately 0.6 to 0.8. This manifests the

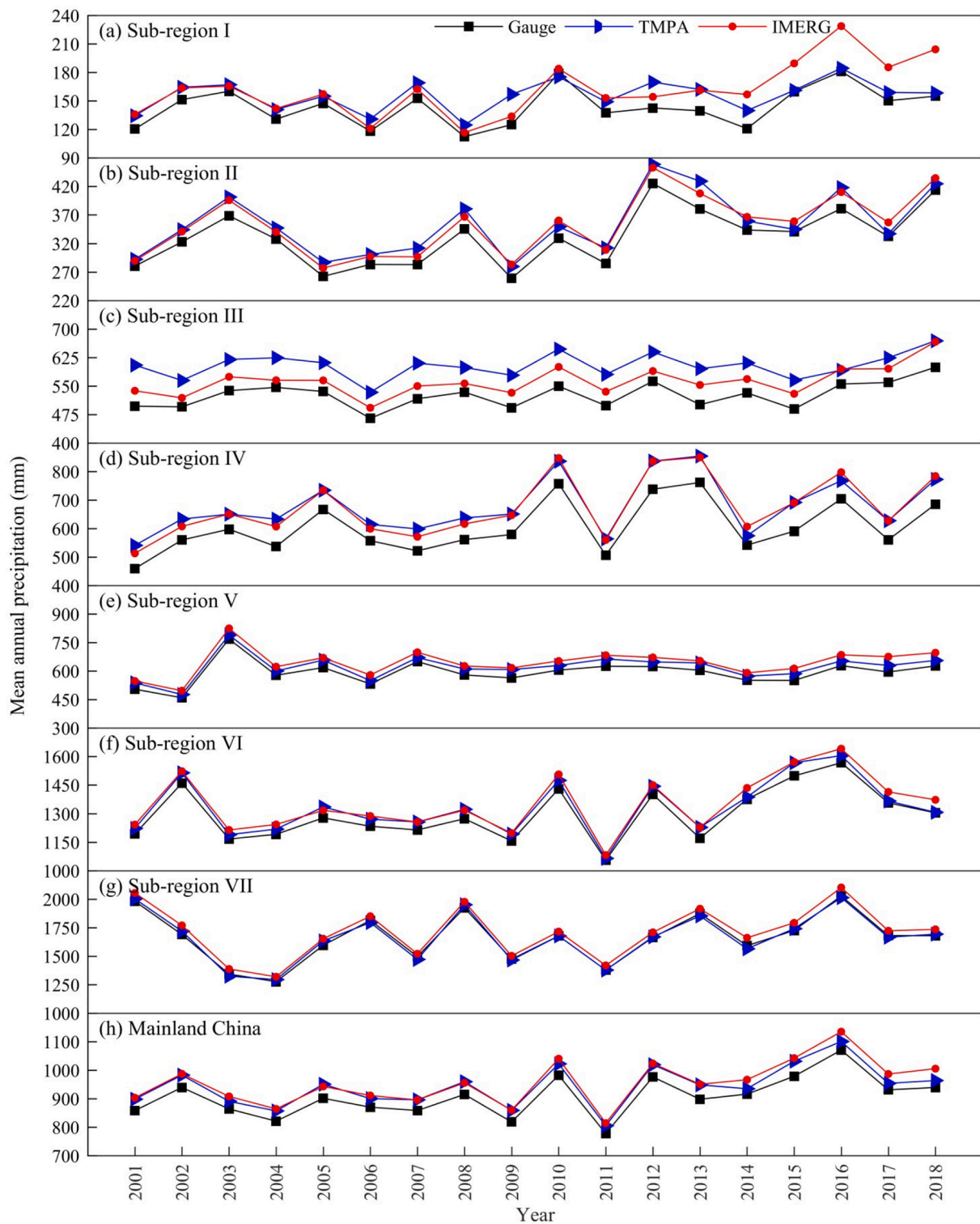


Fig. 10. Comparison of the temporal variations in the observed and TMPA- and IMERG-retrieved mean annual Pr (from 2001 to 2018) in different subregions and mainland China.

feasibility of using the calibrated a and b parameters to predict the monthly Pr values based on IMERG-retrieved Pr data for the coming future. Furthermore, the validation statistics $RMSE$ was 31.7 mm, RB was 1.5% and R^2 was 0.9, which indicated the prediction was reliable. Since the calibration parameters were interpolated to grid scale based on station scale, the cross-validate of the predicted results was operated, and the NSE was 0.99, the SEE was 10.21, which showed that the

interpolation was viable and minimal error was introduced from the stations to the grids.

The prediction of monthly Pr could be conducted immediately after the newest IMERG Pr data are available. For instance, the prediction result in July 2019 was analyzed in more detail. The accuracy of the predicted Pr data ($RRMSE = 32.6\%$) improved compared with the original released IMERG Pr data ($RRMSE = 35.1\%$), the Pr errors were

Table 2

The performance of IMERG and TMPA precipitation products at the three timescales in different subregions of China.

Item	Timescale	Subregion	I	II	III	IV	V	VI	VII	Mainland China
R ²	Daily	TRMM	0.12	0.35	0.33	0.39	0.42	0.45	0.46	0.45
		IMERG	0.26	0.50	0.43	0.55	0.54	0.54	0.54	0.55
	Monthly	TRMM	0.46	0.86	0.79	0.87	0.86	0.85	0.87	0.88
		IMERG	0.50	0.89	0.83	0.91	0.88	0.87	0.88	0.90
	Annual	TRMM	0.49	0.79	0.70	0.82	0.76	0.83	0.80	0.93
		IMERG	0.40	0.83	0.74	0.88	0.76	0.85	0.80	0.94
RRMSE	Daily	TRMM	5.36	3.96	2.84	3.39	3.52	2.44	2.46	2.92
		IMERG	4.49	3.19	2.31	2.61	2.99	2.09	2.22	2.51
	Monthly	TRMM	1.19	0.51	0.62	0.47	0.48	0.36	0.38	0.44
		IMERG	1.13	0.45	0.53	0.40	0.47	0.32	0.37	0.40
	Annual	TRMM	0.64	0.19	0.33	0.19	0.17	0.14	0.14	0.17
		IMERG	0.68	0.16	0.27	0.17	0.19	0.13	0.14	0.17

narrowed and the spatial coverage could span the entire study area, which was much better than that from interpolating the ground-station-observed Pr data (Fig. 12). The spatial distribution patterns were highly similar, and the range of monthly predicted Pr was narrower after calibration using the original IMERG data (Fig. 12). The map of Fig. 12c is very useful and exhibits high data reliability, for example, for precipitation monitoring or further drought assessment in mainland China.

4. Discussion

Previous studies have conducted performance assessments between ground-observed Pr and satellite-retrieved values for different sites, regions or countries in the world. However, most previous studies applied short-term data. For example, Anjum et al. (2018) compared the TMPA and IMERG products using reference gauge data from 2014 to 2016 over the northern highlands of Pakistan. Wang and Lu (2016) compared GPM Level 3 IMERG and TRMM 3B42V7 daily Pr data from 2014 to 2015 over the Mekong River Basin. Wang et al. (2019) evaluated TRMM 3B42V7 and GPM products from 2014 to 2016 in Guangdong Province, China. Su et al. (2019) compared IMERG and TMPA products against a relatively dense gauge network from 2014 to 2018 over mainland China. Fei et al. (2018) conducted a comparative analysis on the quality of the TMPA 3B42V7 and the IMERG final run V05 Pr products and applied them in the Yellow River source region from 2014 to 2016. Tang et al. (2016) evaluated Day-1 IMERG and TMPA Version-7 legacy products over mainland China from April to December in 2014. This study investigated the spatiotemporal performance of the IMERG and TMPA Pr datasets at multiple timescales for 20 years of Pr data in 7 subregions of China. The long time series made our results more convincing than the results of previous research.

The reliability and accuracy of satellite data are affected by the climatic and geographic conditions (Zambrano-Bigiarini et al., 2017; Hussain et al., 2018) as well as the seasons (Darand et al., 2017). Hence, in this study we divided China into 7 different subregions (Zhang, 1983), and analyzed the performance of two products in diverse subregions and seasons in great details, and found that two products performed generally good but worse in subregions I and III. Compared with the other subregions, the annual Pr in sub-region I (Mid-temperate arid) was obviously lower (Table 1), light Pr events occurred frequently and daily average Pr was < 5 mm (Fig. 4), therefore, low Pr events would affect the accuracy of the satellite data (Gao and Liu, 2012). Fortunately, the latest IMERG improved this issue than TMPA, which retained the original advantage. For subregion III (Plateau sub-frozen semiarid) which contained complex terrain, the accuracy of both IMERG and TMPA products were reduced for algorithm defect and aerosol (Kim et al., 2017), and the high elevation also strongly affected the products precision (Andrés Navarro et al., 2020). Furthermore, in winter and summer, two products exhibited relative poor performance due to the higher occurrence of convective Pr during the monsoon

season, which caused higher demands on efficient detection of convective Pr (Vide and Olcina, 2001; Kenawy et al., 2015).

Grid-scale satellite-retrieved Pr data and good linear relationship are crucial to the prediction of Pr with an appropriate calibration procedure. Previous studies have also calibrated Pr data using multisource satellite products. Duan and Bastiaanssen (2013) applied geographical differences and geographical ratio analysis for Pr value validation. They found that scaling reduction was further corrected with limited ground station data, and the overall accuracy of the corrected data was improved. Cheema and Bastiaanssen (2012) calibrated the TRMM Pr dataset and compared RA (regression analysis) and GDA (geographic differential analysis) and found that the two methods were good for calibrating the satellite datasets. Previous research only calibrated or assessed the performance of the satellite data; however, they seldom used the results for Pr data prediction. In this research, we calibrated the IMERG-retrieved monthly Pr data and further predicted the corrected IMERG dataset.

Among the various satellite-gauge merging approaches, scaling method was frequently adopted as a core idea (Vila et al., 2009; Tesfagiorgis et al., 2011; Jongjin et al., 2016). It computed the additive or multiplicative deviation between the satellite- and gauge-based Pr to rescale the original satellite Pr. This method would fail to work without the synchronous reference data, and insufficiently made use of the valuable information in long-term data. Compared with it, the linear regression-based method which we have applied overcame these defects well. The linear relationship connected the historical stations-observed data with simultaneous satellite data to get the function parameters used to calculate the corrected or predicted satellite Pr. Furthermore, higher computational efficiency and convenience of operation were also vital factors in determining whether the method would be widely adopted. The linear regression-based method was simple, convenient to execute and efficient, it only needed to calculate once to obtain the correction or prediction parameters, then based on the newly released satellite data, the Pr could be predicted directly. With these advantages, it could be chosen as an appropriate method for correcting or predicting Pr based on satellite data.

The results demonstrated that the IMERG data were more suitable than TMPA data for application over China, even in Northwest China (subregion I) and the Qinghai-Tibet Plateau (subregion III), where gauge stations are sparse. The correction of the Pr data to the area overcame this shortage and had several potential applications in hydrology modeling, meteorological and agricultural drought analysis, weather forecasting, climate prediction, and even crop growth modeling. Further studies should correct the historical and upcoming IMERG data to the study area (mainland China) and use the long-term data for more research.

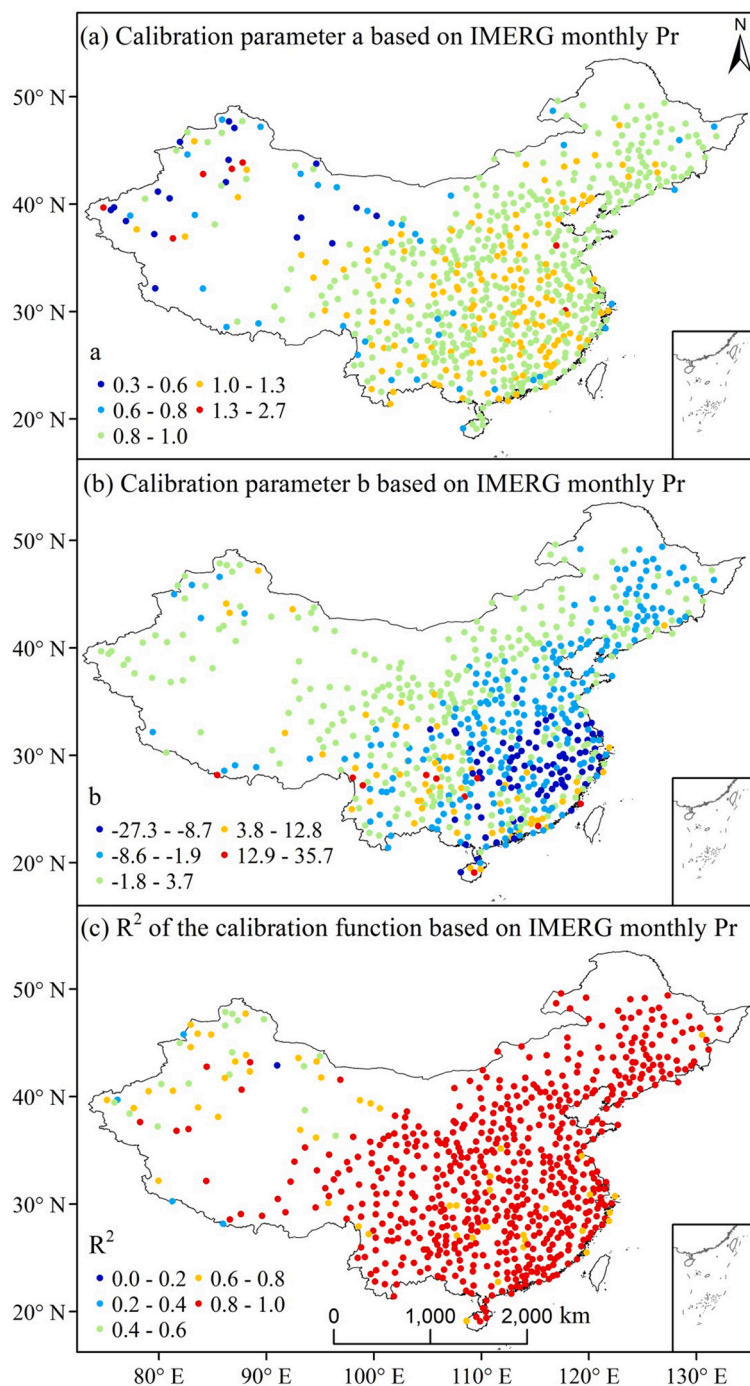


Fig. 11. Spatial distribution of calibration parameters *a* and *b* and the R^2 values of the regression equations based on IMERG monthly Pr from June 2000 to June 2019 in China.

5. Conclusions

The performance of the TMPA- and IMERG-retrieved Pr data was comprehensively assessed with gauge-observed data in 7 subregions and mainland China at the daily, monthly and annual timescales from June 2000 to June 2019. The accuracy of the two satellite products increased with expanding timescales. At certain timescales, IMERG exhibited better performance than TMPA. For each time scale, the worst performance occurred in the mid-temperature arid zone (subregion I), and the best performance occurred in the mid-temperate semihumid

zone (subregion IV). The IMERG products were slightly better than the TMPA products for most subregions.

Both the performance of IMERG and TMPA differed greatly at 12 months, and both exhibited poor performance in dry (December, January and February) or wet (July, August and September) seasons. IMERG performed better than TMPA in most subregions and over mainland China. The predicted map of precipitation in July 2019 achieved higher accuracy than the original IMERG data over China and better reflected the distribution of Pr over China. Therefore, the IMERG product surpassed TMPA and can be adopted by users who need Pr data

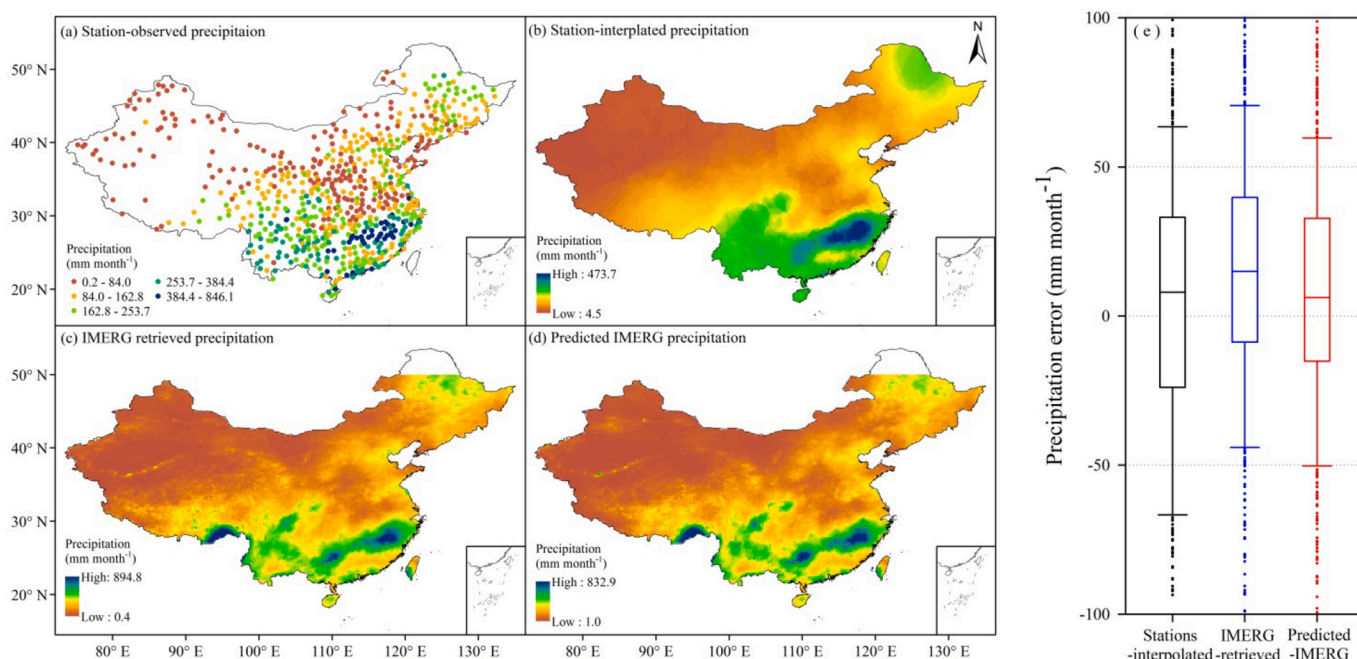


Fig. 12. Spatial distribution of monthly station-observed, station-interpolated, IMERG-retrieved, and IMERG-predicted Pr and boxplots of monthly station-interpolated, IMERG-retrieved, and IMERG-predicted Pr error for July in 2019 in China.

to perform related studies in China.

Author statement

Author Contributions: Conceptualization, Qian Ma and Yi Li; methodology, Hao Feng and Qiang Yu; validation, Yufeng Zou; resources, Fenggui Liu; writing—original draft preparation, Qian Ma; writing—review and editing, Yi Li; funding acquisition, Yi Li; revision, Qian Ma, Yi Li and Bakhtiyor Pulatov. All authors have read and agreed to the published version of the manuscript.

Declaration of Competing Interest

The authors declare that they have no known competing financial interests or personal relationships that could have appeared to influence the work reported in this paper.

Acknowledgments

This research was jointly supported by the National Natural Science Foundation of China (52079114) and the China 111 project (B12007). We thank the Meteorological Data Sharing Service Network in China for sharing the weather data.

Appendix A. Supplementary data

Supplementary data to this article can be found online at <https://doi.org/10.1016/j.atmosres.2020.105304>.

References

- Anjum, M.N., Ding, Y., Shangguan, D., Ahmad, I., Ijaz, M.W., Farid, H.U., Yagoub, Y.E., Zaman, M., Adnan, M., 2018. Performance evaluation of latest integrated multi-satellite retrievals for Global Precipitation Measurement (IMERG) over the northern highlands of Pakistan. *Atmos. Res.* 205, 134–146.
- Anjum, M.N., Ahmad, I., Ding, Y., Shangguan, D., Zaman, M., Ijaz, M.W., ... Yang, M., 2019. Assessment of IMERG-V06 Precipitation Product over Different Hydro-Climatic Regimes in the Tianshan Mountains, North-Western China. *Remote Sensing* 11 (19).
- Ason, Z., Razavi, S., Wheeler, H., Wong, J., 2017. Evaluation of integrated multisatellite retrievals for GPM (IMERG) over southern Canada against ground precipitation

- observations: a preliminary assessment. *J. Hydrometeorol.* 18, 1033–1050.
- Bai, X., Wu, X., Wang, P., 2019. Blending long-term satellite-based precipitation data with gauge observations for drought monitoring: considering effects of different gauge densities. *J. Hydrol.* 577, 124007.
- Cheema, M.J.M., Bastiaanssen, W.G.M., 2012. Local calibration of remotely sensed rainfall from the TRMM satellite for different periods and spatial scales in the Indus Basin[J]. *Int. J. Remote Sens.* 33 (7–8), 2603–2627.
- Chen, C., Chen, Q., Duan, Z., Zhang, J., Mo, K., Li, Z., Tang, G., 2018. Multiscale comparative evaluation of the GPM IMERG v5 and TRMM 3B42 v7 precipitation products from 2015 to 2017 over a climate transition area of China. *Remote Sens.* 10, 944.
- Darand, M., Amanollahi, J., Zandkarimi, S., 2017. Evaluation of the performance of TRMM Multi-satellite Precipitation Analysis (TMPA) estimation over Iran. *Atmos. Res.* 190, 121–127.
- Dinku, T., Ruiz, F., Connor, S.J., Ceccato, P., 2010. Validation and intercomparison of satellite rainfall estimates over Colombia. *J. Appl. Meteorol. Climatol.* 49, 1004–1014.
- Duan, Z., Bastiaanssen, W.G.M., 2013. First results from Version 7 TRMM 3B43 precipitation product in combination with a new downscaling-calibration procedure[J]. *Remote Sens. Environ.* 131, 1–13.
- Ebert, E.E., Janowiak, J.E., Kidd, C., 2007. Comparison of near-real-time precipitation estimates from satellite observations and numerical models. *Bull. Am. Meteorol. Soc.* 88, 47–64.
- Fei, Y., Bing, W., Chunxiang, S., Wei, C., Chongxu, Z., Yi, L., et al., 2018. Evaluation of hydrological utility of imerg final run v05 and tpmv3b42v7 satellite precipitation products in the yellow river source region, China. *Journal of Hydrology* S0022169418304670.
- Gao, Y., Liu, M., 2012. Evaluation of high-resolution satellite precipitation products using rain gauge observations over the Tibetan Plateau. *Hydrol. Earth Syst. Sci. Discuss.* 9.
- GRAVETTER, F.J., WALLNAU, L.B., 2006. *Statistics for the Behavioral Sciences*, 7th Ed. Thomson Wadsworth Publishers, Belmont, CA.
- Gu, H., Yu, Z., Yang, C., Liang, C., Wang, W., Ju, Q., 2010. Modeling for System Services Gained Flow based on UML and Petri Nets. *Water Resources Power* 28 (8), 3–6 (in Chinese).
- Helsel, D.R., Hirsch, R.M., 1992. *Statistical Methods in Water Resources*. Elsevier, Amsterdam.
- Hosseini-Moghari, S.-M., Tang, Q., 2020. Validation of GPM IMERG-V05 and V06 precipitation products over Iran. *J. Hydrometeorol.* D-19-0269.1.
- Hou, A.Y., Kakar, R.K., Neeck, S., Azarbarzin, A.A., Kummerow, C.D., Kojima, M., Oki, R., Nakamura, K., Iguchi, T., 2014. The global precipitation measurement mission. *Bull. Am. Meteorol. Soc.* 95, 701–722.
- Huffman, G.J., Adler, R.F., Bolvin, D.T., Gu, G., Nelkin, E.J., Bowman, K.P., Hong, Y., Stocker, E.F., Wolff, D.B., 2007. The TRMM Multi-satellite Precipitation Analysis: Quasi-Global, Multi-Year, Combined-Sensor Precipitation estimates at Fine Scale. *J. Hydrometeorol.* 8 (1) 38–55. PDF available at: ftp://meso.gsfc.nasa.gov/agnes/huffman/papers/TMPA_jhm_07.pdf.gz.
- Huffman, G.J., Adler, R.F., Bolvin, D.T., Nelkin, E.J., 2010. The TRMM Multi-satellite Precipitation Analysis (TMPA). Chapter 1 in *Satellite Rainfall Applications for Surface Hydrology*, F. Hossain and M. Gebremichael, Eds. Springer Verlag, ISBN: 978-90-481-2914-0, 3–22.
- Hussain, Y., Satgé, F., Hussain, M.B., et al., 2018. Performance of CMORPH, TMPA, and

- PERSIANN rainfall datasets over plain, mountainous, and glacial regions of Pakistan. *Theor. Appl. Climatol.* 131, 1119–1132.
- Jiang, S., Ren, L., Yong, B., Yuan, F., Gong, L., Yang, X., 2014. Hydrological evaluation of the TRMM multi-satellite precipitation estimates over theMishui basin. *Adv. Water Sci.* 25 (5), 641–649 (in Chinese).
- Jin, X., Shao, H., Zhang, C., Yan, Y., 2016. The applicability evaluation of three satellite products in Tianshan mountains. *J. Natural Resources (in Chinese)* 31, 2074–2085.
- Jongjin, B., Jongming, P., Dongreol, R., Minha, C., 2016. Geospatial blending to improve spatial mapping of precipitation with high spatial resolution by merging satellite-based and ground-based data. *Hydrological. Processes* 30 (16), 2789–2803.
- Kenawy, A.E., Lopezmoreno, J.I., McCabe, M.F., et al., 2015. Evaluation of the TMPA-3B42 precipitation product using a high-density rain gauge network over complex terrain in northeastern Iberia. *Glob. Planet. Chang.* 188–200.
- Kidd, C., Huffman, G., 2011. Global precipitation measurement. *Meteorol. Appl.* 18, 334–353.
- Kim, K., Park, J., Baik, J., et al., 2017. Evaluation of topographical and seasonal feature using GPM IMERG and TRMM 3B42 over Far-East Asia[J]. *Atmos. Res.* 95–105.
- Kirschbaum, D.B., Huffman, G.J., Adler, R.F., Braun, S., Garrett, K., Jones, E., McNally, A., Skofronick-Jackson, G., Stocker, E., Wu, H., Zaitchik, B.F., 2017. NASA's remotely sensed precipitation: a reservoir for applications users. *Bull. Am. Meteorol. Soc.* 98, 1169–1184.
- Kummerow, C., Barnes, W., Kozu, T., Shiue, J., Simpson, J., 1998. The Tropical Rainfall measuring Mission (TRMM) sensor package. *J. Atmos. Ocean. Technol.* 15, 809–817.
- Kummerow, C., Simpson, J., Thiele, O., Barnes, W., Chang, A.T.C., Stocker, E., Adler, R.F., Hou, A., Kakar, R., Wentz, F., Ashcroft, P., Kozu, T., Hong, Y., Okamoto, K., Iguchi, T., Kuroiwa, H., Im, E., Haddad, Z., Huffman, G., Ferrier, B., Olson, W.S., Zipser, E., Smith, E.A., Wilheit, T.T., North, G., Krishnamurti, T., Nakamura, K., 2000. The status of the tropical rainfall measuring mission (TRMM) after two years in orbit. *J. Appl. Meteorol.* 39, 1965–1982.
- Li, R., Wang, K., Qi, D., 2018. Validating the integrated multisatellite retrievals for global precipitation measurement in terms of diurnal variability with hourly gauge observations collected at 50,000 stations in China. *J. Geophys. Res.-Atmos.* 123, 10,423–410,442.
- Lin, A., Wang, X.L., 2011. An algorithm for blending multiple satellite precipitation estimates with in situ precipitation measurements in Canada. *J. Geophys. Res.-Atmos.* 116 (D21).
- Liu, J., Chen, R., Qin, W., Yang, Y., 2011. Study on the vertical distribution of precipitation in mountations regions using TRMM data. *Adv. Water Sci.* 22 (4), 447–454 (in Chinese).
- Liu, J., Du, J., Yang, Y., et al., 2020. Evaluating extreme precipitation estimations based on the GPM IMERG products over the Yangtze River Basin, China. *Geomat. Natural Hazards Risk* 11 (1), 601–618.
- Ma, L., Zhao, L., Tian, L.-M., Yuan, L.-M., Xiao, Y., Zou, D.-F., Qiao, Y.-P., 2019. Evaluation of the integrated multi-satellite retrievals for global precipitation measurement over the Tibetan Plateau. *J. Mt. Sci.* 16, 1500–1514.
- Ma, Y., Tang, G., Long, D., Yong, B., Zhong, L., Wan, W., Hong, Y., 2016. Similarity and error inter comparison of the GPM and its predecessor-TRMM Multisatellite Precipitation Analysis using the best available hourly gauge network over the Tibetan Plateau. *Remote Sens.* 8, 569.
- Macharia, J.M., Ngetich, F.K., Shisanya, A., 2020. Comparison of satellite remote sensing derived precipitation estimates and observed data in Kenya. *Agricultural and Forest Meteorology*.
- Mahmoud, M.T., Al-Zahrani, M.A., Sharif, H.O., 2018. Assessment of global precipitation measurement satellite products over Saudi Arabia. *J. Hydrol.* 559, 1–12.
- NASH, J.E., SUTCLIFFE, J.V., 1970. River flow forecasting through conceptual models part 1—a discussion of principles. *J. Hydrol.* 10, 282–290.
- Navarro, Andrés, García-Ortega, Eduardo, Merino, Andrés, Sánchez, José Luis, Tapiador, Francisco J., 2020. Orographic biases in IMERG precipitation estimates in the Ebro River basin (Spain): the effects of rain gauge density and altitude. *Atmos. Res.* 244.
- Prakash, S., Mitra, A.K., AghaKouchak, A., Pai, D., 2015. Error characterization of TRMM Multisatellite Precipitation Analysis (TMPA-3B42) products over India for different seasons. *J. Hydrol.* 529, 1302–1312.
- Shen, Y., Xiong, A., Wang, Y., Xie, P., 2010. Performance of high-resolution satellite precipitation products over China. *J. Geophys. Res.-Atmos.* 115.
- Su, F., Hong, Y., Lettenmaier, D.P., 2008. Evaluation of TRMM Multisatellite Precipitation Analysis (TMPA) and its utility in hydrologic prediction in the La Plata Basin. *J. Hydrometeorol.* 9, 622–640.
- Su, J., Lü, Haishen, Ryu, D., Zhu, Y., 2019. The assessment and comparison of tmpa and imerg products over the major basins of mainland China. *Earth Space Sci.* 2019, 6(12).
- Tang, G., Ma, Y., Long, D., Zhong, L., Hong, Y., 2016. Evaluation of GPM Day-1IMERG and TMPA Version-7 legacy products over Mainland China at multiple spatio-temporal scales. *J. Hydrol.* 533, 152–167.
- Tarek, M.H., Hassan, A., Bhattacharjee, J., Choudhury, S.H., Badruzzaman, A.B.M., 2017. Assessment of TRMM data for precipitation measurement in B angladesh. *Meteorol. Appl.* 24, 349–359.
- Tesfagiorgis, K., Mahani, S.E., Krakauer, N.Y., Khanbilvardi, R., 2011. Bias correction of satellite rainfall estimates using a radar-gauge product—a case study in Oklahoma (USA). *Hydrol. Earth Syst. Sci.* 15 (8), 2631–2647.
- Vide, Martin, Olcina, 2001. J. Martin Vide, J., 2001. Olcina Climas y tiempos de España Alianza Editorial, Madrid, pp. 258.
- Vila, D.A., de Goncalves, L.G.G., Toll, D.L., Rozante, J.R., 2009. Statistical evaluation of combined daily gauge observations and rainfall satellite estimates over continental South America. *J. Hydrometeorol.* 10 (2), 533–543.
- Wang, X.L., Lin, A., 2015. An algorithm for integrating satellite precipitation estimates with in situ precipitation data on a pentad time scale. *J. Geophys. Res.-Atmos.* 120 (9), 3728–3744.
- Wang, W., Lu, H., 2016. Evaluation and comparison of newest GPM and TRMM products over Mekong River Basin at daily scale. In, *2016 IEEE International Geoscience and Remote Sensing Symposium (IGARSS)* (pp. 613–616): IEEE.
- Wang, Z., Zhong, R., Lai, C., et al., 2017. Evaluation of the GPM IMERG satellite-based precipitation products and the hydrological utility. *Atmos. Res.* 196 151–163.
- Wang, D., Wang, X., Liu, L., Wang, D., Huang, H., Pan, C., 2019. Evaluation of TMPA 3B42V7, GPM IMERG and CMPA precipitation estimates in Guangdong Province, China. *Int. J. Climatol.* 39, 738–755.
- Wehbe, Y., Ghebreyesus, D., Temimi, M., Milewski, A., Al Mandous, A., 2017. Assessment of the consistency among global precipitation products over the United Arab Emirates. *J. Hydrol. Reg. Stud.* 12, 122–135.
- Wu, Z., Zhang, Y., Sun, Z., Lin, Q., He, H., 2018. Improvement of a combination of tmpa (or imerg) and ground-based precipitation and application to a typical region of the East China plain. *Ence of the Total Environment*, 640-641(NOV.1), 1165–1175.
- Yang, R., Gao, G., Zhang, J., 2019. Research of TRMM3B43 satellite precipitation data applicability in Beijing-Tianjing-Hebei region. *J. Glaciol. Geocryol.* 41 (4), 1–8 (in Chinese).
- Yang, X., Lu, Y., Tan, M.L., Li, X., Wang, G., He, R., 2020. Nine-Year Systematic Evaluation of the GPM and TRMM Precipitation Products in the Shuishui River Basin in East-Central China. *Remote Sens.* 12, 1042.
- Yong, B., Chen, B., Tian, Y., Yu, Z., Hong, Y., 2016. Error-component analysis of TRMM-based multi-satellite precipitation estimates over mainland China. *Remote Sens.* 8, 440.
- Zambrano-Bigiarini, M., Nauditt, A., Birkel, C., Verbist, K., Ribbe, L., 2017. Temporal and spatial evaluation of satellite-based rainfall estimates across the complex topographical and climatic gradients of Chile. *Hydrol. Earth Syst. Sci.* 21, 1295–1320.
- Zender, C.S., 2008. Analysis of self-describing gridded geoscience data with netCDF Operators (NCO)[J]. *Environ. Model. Softw.* 23 (10–11), 1338–1342.
- Zhang, S., 1983. A new scheme for comprehensive phisical regionlization in China. *Acta Geograph. Sin.* 38 (1), 1–10 (in Chinese).
- Zhang, Z., Chen, X., Xu, C.-Y., Yuan, L., Yong, B., Yan, S., 2011a. Evaluating the non-stationary relationship between precipitation and streamflow in nine major basins of China during the past 50 years. *J. Hydrol.* 409, 81–93.
- Zhang, Q., Sun, P., Chen, X., & Chen, X., 2011b. Water Resources in China from 1956 to 2000: Changing Properties, Causes and Implications. *Sci. Geogr. Sin.*, 31(12), 1430–1436. (in Chinese).
- Zhao, H., Yang, S., Wang, Z., et al., 2015. Evaluating the suitability of TRMM satellite rainfall data for hydrological simulation using a distributed hydrological model in the Weihe River catchment in China. *J. Geogr. Sci.* 25, 177–195.
- Zhao, H., Yang, B., Yang, S., Huang, Y., Dong, G., Bai, J., Wang, Z., 2018. Systematical estimation of GPM-based global satellite mapping of precipitation products over China. *Atmos. Res.* 201, 206–217.